Cleft Alveolus Reconstruction Using a Three-Dimensional Printed Bioresorbable Scaffold With Human Bone Marrow Cells

Article *in* Journal of Craniofacial Surgery · July 2018

DOI: 10.1097/SCS.0000000000004747

CITATION
1

READS
90

5 authors, including:

Won Soo Yun
Korea Polytechnic University
39 PUBLICATIONS **338** CITATIONS
SEE PROFILE

Ui-Lyong Lee
Chung-Ang University
27 PUBLICATIONS **139** CITATIONS
SEE PROFILE

Cleft Alveolus Reconstruction Using a Three-Dimensional Printed Bioresorbable Scaffold With Human Bone Marrow Cells

Geunseon Ahn, MS, Jeong-Seok Lee, BS,† Won-Soo Yun, PhD,† Jin-Hyung Shim, PhD,† and Ui-Lyong Lee, DDS, MSD‡*

Abstract: Bone tissue engineering technology based on scaffold has been applied for cleft lip and palate treatment. However, clinical applications of patient-specific three-dimensional (3D) scaffolds have rarely been performed. In this study, a clinical case using patient-specific 3D-printed bioresorbable scaffold with bone marrow stromal cells collected from iliac crest in the operating room has been introduced. At 6-month after transplantation, the bone volume of the newly regenerated bone was approximately 45% of the total defect volume. Bone mineral density of the newly regenerated bone was about 75% compared to the surrounding bone. The Hounsfield unit value was higher than that of cancellous maxillary alveolar bone and lower than that of the cortical maxillary alveolar bone. Bone-marrow-derived mesenchymal stem cells-seeded 3D-printed patient-specific polycaprolactone scaffolds offer a promising alternative for alveolar cleft reconstruction and other bony defects.

Key Words: Bioresorbable scaffold, cleft alveolus reconstruction, human bone marrow cells, three-dimensional printing

(*J Craniofac Surg* 2018;00: 00–00)

The current method for treating cleft alveolus is an iliac crest autogenous bone graft. However, this method may cause donor-site morbidity, including postoperative pain, sensory abnormalities, ambulatory difficulty, risk of infection, and contour defects.[1] To overcome these limitations, implants that are effective in bone regeneration can be used as an alternative.[2–5] With the increasing use of cone-beam computed tomography (CBCT) technology, computer-aided design/computer-aided manufacturing, and 3D printing technology, patient-specific 3D-printed scaffolds are available for oral and maxillofacial surgery.[6–11]

Three-dimensional printing technology can be used to produce complex shapes. Nonbiodegradable scaffolds, made of titanium or polyetherketoneketone, have been fabricated with 3D printing technology.[12–15] However, the grafted nonbiodegradable scaffolds are permanent and may cause inflammation and infection at the implanted site.[16,17] Therefore, a scaffold with biocompatibility, biodegradability, and customized shape would be useful for clinical applications.

Due to their ability to self-renew and differentiate into osteogenic lineage, mesenchymal stem cells (MSCs) from bone marrow are used for regeneration of bone.[18] Transplanting a bone marrow aspirate allows the cells to be processed directly in the operating room without the need for a laboratory or centrifugation.[19] Furthermore, it can promote vascularization, since the aspirate contains angiogenic factors.

Here, we report the world's first case of regeneration of an alveolar cleft defect treated with a patient-specific 3D-printed bioresorbable polycaprolactone (PCL) scaffold seeded with iliac bone marrow cells. This case suggests that cell seeded 3D-printed scaffolds offer a tissue engineering alternative for alveolar cleft reconstruction, and other bony defects.

METHODS

Patient

A 10-year-old Korean boy with a history of previously repaired unilateral cleft lip and palate presented with a cleft alveolus and an oronasal fistula. The patient's weight (27.6 kg) and height (132 cm) were less than those of contemporaries of the same age, and the patient's parents were concerned about a decline in growth related to harvesting bone from the iliac crest. To avoid an autologous bone graft, we established a surgical plan to graft a 3D-printed PCL scaffold for this patient who presented with an irregularly shaped defect. We have received consent from the patient's parent to proceed with the procedure using 3D-printed PCL scaffold.

Fabrication of 3D-Printed Bioresorbable Scaffold

The CBCT was obtained while the patient was placed in the upright position. The Frankfurt horizontal plane was parallel to the floor and the patient was asked to maintain centric occlusion. Data from the maxillofacial regions were obtained with a 0.4-mm voxel size and 512 × 512 matrices using 120 kVp, 11 mA, 17.8 seconds of scan time, and 12-inch detector field. Data were stored in the Digital Imaging and Communications in Medicine format and reconstructed into 3D bone images using Mimics software (Materialise,

From the *Research Institute, T&R Biofab Co Ltd; †Department of Mechanical Engineering, Korea Polytechnic University, Gyeonggi-do; and ‡Department of Oral & Maxillofacial Surgery, Dental Center, Chung-Ang University Hospital, Seoul, Republic of Korea.

Received January 15, 2018.
Accepted for publication May 20, 2018.

Address correspondence and reprint requests to Ui-Lyong Lee, DDS, MSD, Department of Oral & Maxillofacial Surgery, Dental Center, Chung-Ang University Hospital, 224-1 Heukseok-dong, Dongjak-ku, Seoul 06973, Republic of Korea; E-mail: davidjoy76@gmail.com, Jin-Hyung Shim, PhD, Department of Mechanical Engineering, Korea Polytechnic University, 237 Sangidaehak-ro, Siheung-si, Gyeonggi-do 15073, Republic of Korea; E-mail: happyshim@kpu.ac.kr
Geunseon Ahn and Jeong-Seok Lee contributed equally to this work.

This work was supported by Priority Research Centers Program through the National Research Foundation of Korea (NRF) funded by the Ministry of Education (NRF-2017R1A6A1A03015562).
The authors report no conflicts of interest.

ISSN: 1049-2275
DOI: 10.1097/SCS.0000000000004747

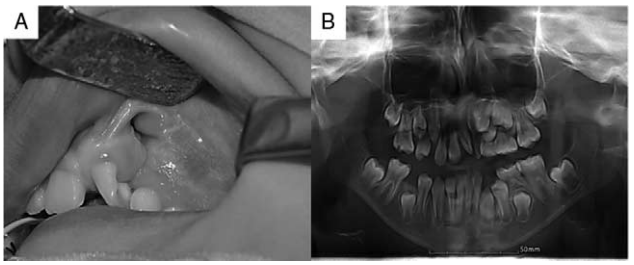

FIGURE 1. Photograph and radiograph of the patient before transplantation. (A) Intraoral photographic view and (B) panoramic radiographic view.

Leuven, Belgium). A customized model of the defect was made using commercial 3D medical image editing software (Materialise). The defect-customized 3D model was converted into printing path data using a printing path generation algorithm. Medical-grade PCL (Evonik Industry, Pharma Polymers, Essen, Germany) was used to fabricate the customized defect scaffold. A micro-extrusion-based 3D bioprinter (T&R Biofab Co, Ltd, Siheung, Republic of Korea), located in a Good Manufacturing Product facility and approved by the Korean Food and Drug Administration, was used for fabrication of the scaffold using a layer-by-layer process. The 3D bioprinter was equipped with a steel syringe containing the PCL material, and the syringe was maintained at 110°C while dispensing of the molten PCL.

The morphology of the printed scaffold was observed under a field emission scanning electron microscope (S-4700; HITACHI, Tokyo, Japan) operated at 15 kV. The images were analyzed to confirm the internal structure. The implant was sterilized by gamma rays prior to transplantation.

Surgical Procedure

After local anesthesia, an incision was made in the lining mucosa of the oronasal fistula and extended vertically along the edge of the alveolar cleft. The mucosa of the palate was elevated for palatal closure. A palatal flap with a posterior release was used for unstressed suture of cleft bone graft. The nasal cavity and palatal side were closed with 4-0 vicryl. Twenty milliliter of bone marrow aspirate was collected from the posterior iliac crest. The bone marrow aspirate was embedded on the scaffold and incubated for 20 minutes before transplantation. The scaffold seeded with bone-marrow-derived MSCs (BMSCs) was transplanted into the alveolar defect. After confirming that the scaffold was located well in the alveolar ridge, 2 holes were drilled using a round bur on the alveolar wall of alveolar ridge. Then, the scaffold was fixed with 2-hole titanium mini-plate with 2 mm in thickness (Jeil Medical Co, Seoul, Republic of Korea) and mini-screws with 2 mm in diameter and 6 mm in length (Jeil Medical Co).

Measurement of Bone Volume Fraction and Bone Mineral Density

To confirm new bone formation after transplantation, radiodensity analysis of CT images was used to measure bone volume (BV) and density. The Hounsfield unit (HU) scale was used to compare volume and density at different time points. The region of interest was identified from preoperative and 6 months postoperative CT images. The applied threshold was 226 HU for measuring the bone mineral density of newly regenerated bone and the bone volume fraction (BV/total defect volume [TV]), which is a ratio of the segmented BV to the TV.

RESULTS

Preoperative images show the congenital alveolar cleft defect (Fig. 1A). The lateral incisor was missing and approximately two-thirds of the canine tooth root was formatted (Fig. 1B). The defect and placement of the 3D scaffold model are shown in Figure 2 A and B; Figure 2C and D show the scaffold model. The line width and pore size of the fabricated scaffold were 300 and 300 μm, respectively (Fig. 2E). The fabricated scaffold had lattice-type pore, the calculated porosity was about 50%, and the pores were fully interconnected.

For transplantation of the 3D-printed scaffold, a periosteal elevator was used to elevate the mucosa in the cleft and completely expose the bony wall (Fig. 3A). The BMSCs were embedded in the scaffold before transplantation (Fig. 3B). The BMSC-embedded scaffold was grafted into the alveolar cleft defect and immobilized with a mini-screw and a mini-plate (Fig. 3C). A lateral sliding flap was elevated as far as possible with a wide base at the cleft and used

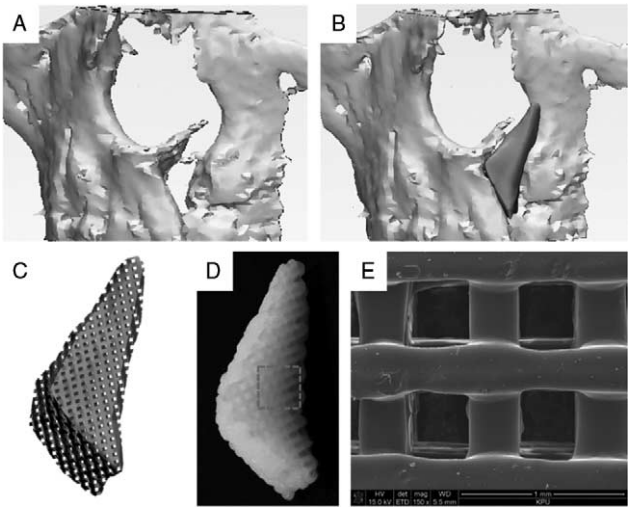

FIGURE 2. Fabrication of patient-specific 3D-printed scaffold. (A) 3D-reconstructed defect model, (B) defect-customized scaffold (purple), (C) porous structure of the scaffold, (D) 3D-printed scaffold, and (E) scanning electron micrograph image of the scaffold.

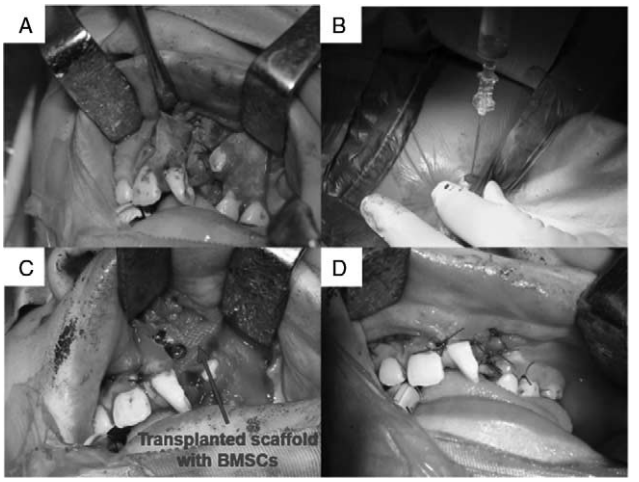

FIGURE 3. Surgical procedure. (A) Exposure of the cleft bony wall, (B) collection of bone-marrow-derived mesenchymal stem cells (BMSCs) from the posterior iliac crest, (C) transplantation of the scaffold with BMSCs, (D) suturing of the attached gingiva.

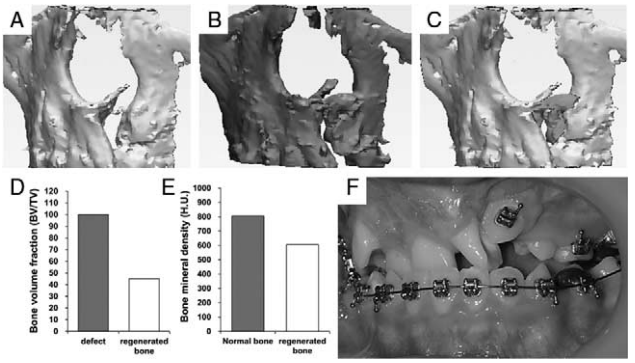

FIGURE 4. Postoperative results. (A) Defect model, (B) 3D reconstructed computed tomography data 6 months after transplantation, (C) a merged image of the preoperative scaffold (purple) and the newly regenerated bone (green), (D) bone volume fraction, (E) bone mineral density, and (F) closing the oronasal fistula.

to close the oral layer. The adjacent attached gingiva approximated the alveolar cleft area and was sutured without tension (Fig. 3D).

Four months after surgery, a portion of the plate that fixed the PCL was exposed, and we removed the plate and screws. The oronasal fistula was closed, and a bony bridge had developed in the alveolar defect. The left maxillary canine had erupted, and no additional surgery was planned. When compared to the initial defect (Fig. 4A), 6 months after surgery, the new bone was evident at the transplanted site (Fig. 4B). Merged images of the preoperative scaffold (purple) and the newly regenerated bone (green) are shown in Figure 4C. In quantitative analysis, the BV of the newly regenerated bone was 45% of the total defect volume (Fig. 4D). Bone mineral density of the newly regenerated bone was about 604.8 HU, compared with about 806 HU for the normal bone surrounding the defect (Fig. 4E). The left maxillary canine erupted, and orthodontic treatment was started 8 months after surgery (Fig. 4F).

DISCUSSION

Standard reconstructive techniques for bony critical size defects include autologous grafts, nonvascularized bone grafts, and vascularized free flaps. These techniques involve donor-site morbidity and are time-consuming procedures to shape the graft to the complex 3D defect configuration.[20] In tissue engineering, a biocompatible and bioresorbable 3D porous scaffold is essential for stable settlement and maturity of cells and tissues.[21,22] In addition, the use of 3D printing technology in scaffold fabrication is easy, fast, affordable, and allows customization of porosity and shape with biocompatible materials.[23,24] In this study, we adapted in-house 3D printer using extrusion-based dispensing method to print a defect-customized scaffold and successfully prepared the scaffold for the alveolar bone defect. We used a PCL scaffold that is approved by the Korean Ministry of Food and Drug Safety for the clinical use. Printed bioresorbable PCL is suitable for bone tissue engineering applications because it can fabricated with using a 3D printer, is biocompatible, is relatively inexpensive, and degrades slowly.[25] In addition, successful use of a 3D-printed PCL airway splint for the treatment of tracheobronchomalacia has recently been reported.[26]

The MSCs have anti-inflammatory and anti-fibrotic properties.[27] Bone regeneration of transplanted BMSCs is enhanced due to their capacity of bone tissue regeneration and angiogenesis.[28–31] To induce effective bone regeneration, BMSCs extracted from the patient's iliac crest were added to the scaffold. Six months after surgery, a substantial amount of new bone was observed at the defect site. Although the mean density was lower than that of the normal bone surrounding the defect, the HU value was higher than that of cancellous maxillary alveolar bone, and lower than that of the cortical maxillary alveolar bone. Active in-growth and regeneration of bone tissue into the scaffold can be attributed to the fully interconnected pores of the printed scaffold, the fixation technique with plate and screws, the high osteogenic capacity of the cleft defect, and the bone regeneration potential of BMSCs. In conclusion, BMSC-seeded 3D-printed patient-specific PCL scaffolds offer a promising alternative for alveolar cleft reconstruction and other bony defects. On the contrary, long-term observation of this case is required, and use of new biomaterial such as blended PCL and tricalcium phosphate scaffold, which is a well-known bone conductive material,[5] will be undertaken. Moreover, further studies are needed on optimal cell seeding concentration.

REFERENCES

1. Khojasteh A, Kheiri L, Motamedian SR, et al. Regenerative medicine in the treatment of alveolar cleft defect: a systematic review of the literature. *J Craniomaxillofac Surg* 2015;43:1608–1613
2. Jazayeri H, Dashtimoghadam E, Rasoulianbroujeni M, et al. 3-D printed PCL/halloysite scaffolds for craniomaxillofacial bone regeneration. *Dent Mater* 2016;32:e57
3. Liu Y, Lim J, Teoh S-H. Review: development of clinically relevant scaffolds for vascularised bone tissue engineering. *Biotechnol Adv* 2013;31:688–705
4. Park Y-W, Lee J-H. Use of mandibular chin bone for alveolar bone grafting in cleft patients. *Maxillofac Plast Reconstr Surg* 2016;38:45
5. Shim J-H, Won J-Y, Sung S-J, et al. Comparative efficacies of a 3D-printed PCL/PLGA/-TCP membrane and a titanium membrane for guided bone regeneration in beagle dogs. *Polymers* 2015;7:2061–2077
6. Goh BT, Chanchareonsook N, Tideman H, et al. The use of a polycaprolactone-tricalcium phosphate scaffold for bone regeneration of tooth socket facial wall defects and simultaneous immediate dental implant placement in *Macaca fascicularis*. *J Biomed Mater Res A* 2014;102:1379–1388
7. Goh BT, Teh LY, Tan DBP, et al. Novel 3D polycaprolactone scaffold for ridge preservation-a pilot randomised controlled clinical trial. *Clin Oral Implants Res* 2015;26:271–277
8. Jadhav C, Cunneen S. Three-dimensional printing technology for medial orbital wall fractures. *J Craniofac Surg* 2015;26:e799–e800
9. Jo Y-Y, Kim S-G, Kim M-K, et al. Mandibular reconstruction using a customized three-dimensional titanium implant applied on the lingual surface of the mandible. *J Craniofac Surg* 2018;29:415–419
10. Rasperini G, Pilipchuk S, Flanagan C, et al. 3D-printed bioresorbable scaffold for periodontal repair. *J Dent Res* 2015;94(Suppl):153S–157S
11. Wauters LD, San Miguel-Moragas J, Mommaerts MY. Classification of computer-aided design-Computer-aided manufacturing applications for the reconstruction of cranio-maxillo-facial defects. *J Craniofac Surg* 2015;26:2329–2333
12. Choi JW, Kim N. Clinical application of three-dimensional printing technology in craniofacial plastic surgery. *Arch Plast Surg* 2015;42:267–277
13. Misch CM. Bone augmentation of the atrophic posterior mandible for dental implants using rhBMP-2 and titanium mesh: clinical technique and early results. *Int J Periodontics Restorative Dent* 2011;31:581–589
14. Rotaru H, Schumacher R, Kim S-G, et al. Selective laser melted titanium implants: a new technique for the reconstruction of extensive zygomatic complex defects. *Maxillofac Plast Reconstr Surg* 2015;37:1
15. Zembic A, Sailer I, Jung RE, et al. Randomized-controlled clinical trial of customized zirconia and titanium implant abutments for single-tooth implants in canine and posterior regions: 3-year results. *Clin Oral Implants Res* 2009;20:802–808
16. Böstman O, Pihlajamäki H. Clinical biocompatibility of biodegradable orthopaedic implants for internal fixation: a review. *Biomaterials* 2000;21:2615–2621
17. Younis I, Gault D, Sabbagh W, et al. Patient satisfaction and aesthetic outcomes after ear reconstruction with a Branemark-type, bone-anchored, ear prosthesis: a 16 year review. *J Plast Reconstr Aesthet Surg* 2010;63:1650–1655

18. Jäger M, Herten M, Fochtmann U, et al. Bridging the gap: bone marrow aspiration concentrate reduces autologous bone grafting in osseous defects. *J Orthop Res* 2011;29:173–180
19. Veronesi F, Giavaresi G, Tschon M, et al. Clinical use of bone marrow, bone marrow concentrate, and expanded bone marrow mesenchymal stem cells in cartilage disease. *Stem Cells Dev* 2012;22:181–192
20. Lee UL, Kwon JS, Woo SH, et al. Simultaneous bimaxillary surgery and mandibular reconstruction with a 3-dimensional printed titanium implant fabricated by electron beam melting: a preliminary mechanical testing of the printed mandible. *J Oral Maxillofac Surg* 2016;74:1501e1–1501e15
21. Han L-H, Suri S, Schmidt CE, et al. Fabrication of three-dimensional scaffolds for heterogeneous tissue engineering. *Biomed Microdevices* 2010;12:721–725
22. Garagiola U, Grigolato R, Soldo R, et al. Computer-aided design/computer-aided manufacturing of hydroxyapatite scaffolds for bone reconstruction in jawbone atrophy: a systematic review and case report. *Maxillofac Plast Reconstr Surg* 2016;38:2
23. Curodeau A, Sachs E, Caldarise S. Design and fabrication of cast orthopedic implants with freeform surface textures from 3-D printed ceramic shell. *J Biomed Mater Res A* 2000;53:525–535
24. Temple JP, Hutton DL, Hung BP, et al. Engineering anatomically shaped vascularized bone grafts with hASCs and 3D-printed PCL scaffolds. *J Biomed Mater Res A* 2014;102:4317–4325
25. Shim J-H, Kim SE, Park JY, et al. Three-dimensional printing of rhBMP-2-loaded scaffolds with long-term delivery for enhanced bone regeneration in a rabbit diaphyseal defect. *Tissue Engineering Part A* 2014;20:1980–1992
26. Zopf DA, Hollister SJ, Nelson ME, et al. Bioresorbable airway splint created with a three-dimensional printer. *N Engl J Med* 2013;368:2043–2045
27. Tolar J, Le Blanc K, Keating A, et al. Concise review: hitting the right spot with mesenchymal stromal cells. *Stem Cells* 2010;28:1446–1455
28. Crane JL, Cao X. Bone marrow mesenchymal stem cells and TGF-β signaling in bone remodeling. *J Clin Invest* 2014;124:466–472
29. Knight MN, Hankenson KD. Mesenchymal stem cells in bone regeneration. *Adv Wound Care (New Rochelle)* 2013;2:306–316
30. Robey PG, Kuznetsov SA, Ren J, et al. Generation of clinical grade human bone marrow stromal cells for use in bone regeneration. *Bone* 2015;70:87–92
31. Hwang DY, On SW, Song SI. Bone regenerative effect of recombinant human bone morphogenetic protein-2 after cyst enucleation. *Maxillofac Plast Reconstr Surg* 2016;38:1–6